

Distance-based Tuning of the EKF for Indoor Positioning in WSNs

Alejandro Correa, Marc Barceló, Antoni Morell, José López Vicario

Universitat Autònoma de Barcelona
Telecommunications and Systems Engineering Department
{Alejandro.Corraea, Marc.Barcelo, Antoni.Morell, Jose.Vicario}@uab.cat

Abstract—This work proposes a filtering method for indoor positioning and tracking applications which combines position, speed and heading measurements with the aim of achieving more accurate position estimates both in the short and the long term. We combine all this data using the well-known Extended Kalman Filter (EKF). The particularity in our proposal is that the EKF is configured using the designed statistical covariance matrix tuning method (SCMT), which is based on the the statistical characteristics of the position measurements. Thanks to the SCMT, the EKF is able to efficiently cope with measurements that have different degrees of uncertainty and, therefore, it achieves high accuracy also in the long-term. The system has been validated in a real environment and the results show a reduction in the positioning error of more than 48% when compared to a regular EKF in the tested scenarios.

I. INTRODUCTION

Recently, there has been an increasing interest in the localization and tracking of people in indoor environments. There are many potential applications such as the guidance of people in touring exhibitions, the monitoring of elderly people or the localization of first responders.

Typically, there are three different types of positioning methods, depending on how they obtain the distance between any two nodes. There are methods based on the Angle of Arrival (AoA), methods based on the Time of Arrival (ToA) and methods based on the Received Signal Strength Indicator (RSSI) [1], [2]. Nowadays, ToA methods employing Ultra Wide Band (UWB) signals show encouraging results [3], [4]. Although AoA and ToA methods are potentially superiors in terms of accuracy, RSSI-based positioning methods are used as far as they require no added hardware. Note that this work is based on Wireless Sensor Networks (WSN) where the nodes are low-size, low-cost and with limited computational capabilities.

Nowadays, pure RSSI-based localization methods do not fulfil the accuracy requirements for being used in indoor tracking systems. This is due to the effect of the wireless channel variability on the RSSI measurements. Recently, researchers have shown that the problems of the pure RSSI-based localization methods can be solved using hybrid systems based on RSSI and inertial measurements [5]. In these systems,

the position of the Inertial Measurement Unit (IMU) on the body determines the accuracy of the inertial observations and therefore the overall accuracy of the positioning system. Previous works have shown that the inertial drift can be reduced by placing the IMU on the foot thanks to the Zero-Velocity Update (ZUPT) strategy [6], [7], [8]. However the foot is not a comfortable place for the user to wear a device. Therefore, we focus on hybrid positioning systems that place the IMU in other parts of the body for the sake of user comfortability. Some examples can be found in [9], [10] where the authors propose a Kalman Filter (KF) that combines RSSI from a WSN with inertial measurements from a hip-mounted IMU. Similarly, in [11] the authors use a chest-mounted IMU and an Extended Kalman Filter (EKF). Moreover, in [12] a KF is used for combining inertial and RSSI measurements from a Wi-Fi network. Other authors use Particle Filters (PF) such as in [13] or in [14] where map information is also taken into account.

Currently, far too little attention has been paid to the configuration of the KF on hybrid positioning systems based on inertial and RSSI measurements. In fact, the works in the literature typically manually adjust the KF without considering the statistical characteristics of the measurements [9], [10], [15]. In this work, we analyze the statistical characteristics of the RSSI-based position measurements and we design a method to configure the EKF based on those statistics. In particular, we design a method to configure the measurement noise covariance matrix of the EKF. This method allows to benefit from the high accuracy of the inertial sensors in the short term and, assisted by the RSSI measurements, extend their accuracy over a long period of time.

The rest of this paper is organized as follows: Section II introduces the system architecture. Section III details the designed statistical covariance matrix tuning method while Section IV presents the experimental validation. Finally, the conclusions of the work are presented in Section V.

II. SYSTEM ARCHITECTURE

This work proposes an indoor tracking system based on inertial observations and RSSI measurements from a WSN. The system employs two different types of measurements. On the one hand, the RSSI values of each radio link between

the mobile node and the nodes in the WSN. On the other hand, the inertial measurements from the accelerometer, the magnetometer and the gyroscope. RSSI measurements are preprocessed in order to estimate the position of the mobile node. Inertial measurements are pre-processed as well in order to estimate the speed and heading of the mobile node. These measurements are combined using an EKF with a statistical covariance matrix tuning method. All the techniques and models described in this section have been chosen according to complexity, versatility and acceptance criteria, that is, we selected computationally low-complex (to be implemented in a WSN node) and widely-used solutions in the literature.

First of all, we model the state of a person in a two dimensional space by means of its position and speed,

$$\mathbf{x}^k = [x^k \quad y^k \quad V^k \quad \theta^k]^T \quad (1)$$

where x^k, y^k represents the position in Cartesian coordinates, V^k is the speed modulus and θ^k the speed direction. The movement of the person is defined as a discrete-time dynamic system,

$$\mathbf{x}^k = \mathbf{F}(\theta^{k-1}) \mathbf{x}^{k-1} + \mathbf{v}^k \quad (2)$$

where k is the time step, $\mathbf{F}(\theta^{k-1})$ is the transition matrix and \mathbf{v}^k is a zero mean Gaussian noise with covariance matrix \mathbf{Q} . The transition matrix is a modification of the constant velocity model that takes into account that the velocity is represented in polar coordinates, that is,

$$\mathbf{F}(\theta^k) = \begin{bmatrix} 1 & 0 & T \cos \theta^k & 0 \\ 0 & 1 & T \sin \theta^k & 0 \\ 0 & 0 & 1 & 0 \\ 0 & 0 & 0 & 1 \end{bmatrix} \quad (3)$$

where T is the time period between measurements. Note that we have considered a polar representation of the velocity vector because this approach fits better to the available measurements (speed modulus and heading).

Similarly, let us consider the following relationship between the measurements $\mathbf{z}^k = [\hat{x}_-^k \quad \hat{y}_-^k \quad \hat{V}_-^k \quad \hat{\theta}_-^k]^T$ and the current state \mathbf{x}^k ,

$$\mathbf{z}^k = \mathbf{H}\mathbf{x}^k + \mathbf{w}^k \quad (4)$$

where \mathbf{H} is the measurement matrix (the identity matrix in our case) and \mathbf{w}^k is a zero mean Gaussian noise with covariance matrix \mathbf{R} .

The position measurements ($\mathbf{m}^k = [\hat{x}_-^k \quad \hat{y}_-^k]^T$) are obtained using a Least Square (LS) algorithm which estimates \mathbf{m}^k in order to minimize the overall square error of the distances estimated. The LS can be expressed as the minimization of the cost function J with respect to $\hat{\mathbf{m}}^k$ [16], that is,

$$\min_{\hat{\mathbf{m}}^k} J = \sum_{i \in \mathcal{R}} \left(\hat{d}_{s_i \rightarrow \mathbf{m}^k} - \|s_i - \hat{\mathbf{m}}^k\| \right)^2 \quad (5)$$

where \mathcal{R} is the set of RSSI values available at the k -th time instant and $\hat{d}_{s_i \rightarrow \mathbf{m}^k}$ is the estimated distance between the i -th anchor node and the mobile node.

The speed modulus measurements (\hat{V}_-^k) are obtained as the product of the number of steps per second times the length of

each step. We assume a constant step length (l_{step}) for a user walking in an indoor environment which is adapted for every user. In order to compute the number of steps per second, we compute the modulus of the acceleration and then we filter the modulus using a low pass linear-phase Finite Impulse Response (FIR) filter (order 20 and 3 Hz cut-off frequency) in order to mitigate the higher frequency accelerations that are not of interest [8]. Finally the number of local maximums in the sequence that are above a predefined threshold (N_{max}) is computed and we obtain \hat{V}_-^k as,

$$\hat{V}_-^k = \frac{N_{max}}{T} l_{step} \quad (6)$$

Lastly, the heading measurements ($\hat{\theta}_-^k$) are obtained using a combination of magnetometer and gyroscope measurements. As shown in [13], the combination of both measurements provides an accurate estimate of the heading and mitigates the particular drawbacks associated to each type of sensors. Mathematically, the combination is expressed as [13],

$$\hat{\theta}_-^k = (1 - W) \left(\hat{\theta}^{k-1} + \bar{\omega}^k T \right) + W \hat{\theta}_{mag}^k \quad (7)$$

where W is a weighting factor, $\bar{\omega}^k$ the integration of the gyroscope signal at the k -th period and $\hat{\theta}_{mag}^k$ the heading estimation from the magnetometer signal at time instant k .

The pre-processed measurements are combined using an EKF with a constant velocity kinematic model. In general, the EKF algorithm is divided in two steps: *i*) the prediction step and *ii*) the correction step. In the prediction step, the a priori estimation of the state vector $\hat{\mathbf{x}}_-^{k+1}$ and the state covariance \mathbf{P}_-^{k+1} are updated using the kinematic model,

$$\hat{\mathbf{x}}_-^{k+1} = \mathbf{F}(\theta^k) \hat{\mathbf{x}}^k \quad (8)$$

$$\mathbf{P}_-^{k+1} = \mathbf{M}^k \mathbf{P}^k (\mathbf{M}^k)^T + \mathbf{Q} \quad (9)$$

where \mathbf{M}^k is the Jacobian matrix of the partial derivatives of the model function $\mathbf{F}(\theta^k) \mathbf{x}^k$ with respect to \mathbf{x}^k . In the second step of the method, i.e. the correction step, the previous predictions are corrected thanks to the measurements and the so-called Kalman gain \mathbf{K}^k [17], that is,

$$\mathbf{K}^{k+1} = \mathbf{P}_-^{k+1} \mathbf{H}^T (\mathbf{H} \mathbf{P}_-^{k+1} \mathbf{H}^T + \mathbf{R}^{k+1})^{-1} \quad (10)$$

$$\hat{\mathbf{x}}_-^{k+1} = \hat{\mathbf{x}}_-^{k+1} + \mathbf{K}^{k+1} \left(\mathbf{z}^{k+1} - h \left(\hat{\mathbf{x}}_-^{k+1} \right) \right) \quad (11)$$

$$\mathbf{P}^{k+1} = (\mathbf{I} - \mathbf{K}^{k+1} \mathbf{H}) \mathbf{P}_-^{k+1} \quad (12)$$

Note that in our case $h \left(\hat{\mathbf{x}}_-^{k+1} \right) = \mathbf{H} \hat{\mathbf{x}}_-^{k+1}$. The performance of the EKF depends on the estimation of the measurement noise covariance matrix \mathbf{R}^{k+1} . However this matrix is usually unknown and typically is manually adjusted in the literature [9], [10], [15]. This adjustment is not efficient due to the variations of the statistics of the measurements. For the sake of brevity, we have described in this section only the main ideas of the algorithms. An extended version of this work can be found in [18]. The next section details the designed covariance matrix tuning method that adjusts the EKF based on those statistics.

III. STATISTICAL COVARIANCE MATRIX TUNED EKF (SCMT-EKF)

It is common in hybrid positioning systems that combine RSSI and inertial measurements by means of an EKF to be accurate in the short-term but not in the long-term. In this work we mitigate that increase in the long-term error (due to the inertial drift) by taking into account that some of the position measurements can be more accurate than others. In this section we first analyze the statistics of the measurements and then we adjust the measurement noise covariance matrix of the EKF accordingly.

The position measurements are obtained using a LS algorithm as detailed in Section II. The LS obtains the position from the distance estimations between the mobile node and the anchor nodes (see equation 5). These distance estimations are based on the RSSI of each radio link which we assume that follow a log-distance path loss model [1],

$$RSSI_{s_i \rightarrow \mathbf{m}^k}^k = P_{1m} - 10\alpha \log_{10} d_{s_i \rightarrow \mathbf{m}^k} - \gamma \quad (13)$$

where $RSSI_{s_i \rightarrow \mathbf{m}^k}^k$ is the received power from i -th node, P_{1m} is the received power at 1 meter from the transmitter, α is the path-loss exponent, $d_{s_i \rightarrow \mathbf{m}^k}$ is the distance to the i -th node and $\gamma \sim \mathcal{N}(0, \sigma_\gamma^2)$ models the shadowing effects.

The distance estimation is obtained using the maximum likelihood estimator [19]

$$\hat{d}_{s_i \rightarrow \mathbf{m}^k} = 10^{\frac{RSSI_{s_i \rightarrow \mathbf{m}^k}^k - P_{1m}}{10\alpha}} \quad (14)$$

and it follows a log-normal distribution [19], that is,

$$\ln \hat{d}_{s_i \rightarrow \mathbf{m}^k} \sim \mathcal{N}(\ln d_{s_i \rightarrow \mathbf{m}^k}, \sigma_d^2), \quad (15)$$

where $\sigma_d = (\sigma_\gamma \ln 10) / (10\alpha)$ is the standard deviation. The mean and variance of the distance estimation are:

$$E[\hat{d}_{s_i \rightarrow \mathbf{m}^k}] = d_{s_i \rightarrow \mathbf{m}^k} e^{\sigma_d^2/2} \quad (16)$$

$$\text{Var}[\hat{d}_{s_i \rightarrow \mathbf{m}^k}] = d_{s_i \rightarrow \mathbf{m}^k}^2 e^{2\sigma_d^2} \quad (17)$$

Note that the estimation is biased with a bias straight proportional to the distance. Moreover, the variance of the estimation exhibits an exponential growth with distance. Therefore the estimation of short distances is more reliable than the estimation of long distances. This fact impinges on the position estimations, that is, the position estimations where the mobile node is close to an anchor node are more reliable.

In this work we identify those distance estimations that correspond to a real distance between the anchor node and the mobile node below $d \leq 1$. In these cases, we fix the estimated position of the mobile node to the anchor position, thus committing a maximum error of 1m. Note that this error is below the accuracy of the equivalent method using a regular EKF (2-3m). Our method discriminates the position measurements by comparing the received power with a given threshold, that is, we compare $P_{max} = \max \mathcal{R}$ with a power threshold (P_{Th}).

Taking into account that the variability of the RSSI measurements can lead to errors in the detection of the more

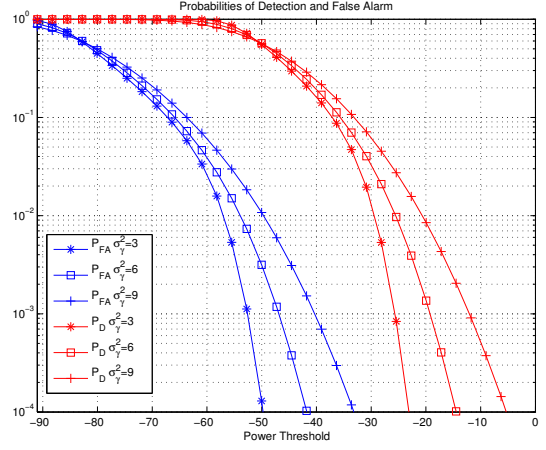


Fig. 1. Probabilities of Detection and False Alarm for different σ_γ^2 .

reliable measurements, we select the power threshold (P_{Th}) based on the probabilities of detection P_D and false alarm P_{FA} . P_D is the probability of having $P_{max} \geq P_{Th}$ given $d \in [d_{min}, 1]$, where $d_{min} \ll 1$ is the minimum distance that assures that we are in the far-field region [20]. Similarly, P_{FA} is the probability of having $P_{max} \geq P_{Th}$ given $d \in (1, d_{max}]$, where d_{max} is the maximum distance between two points in the scenario. Assuming a uniform distribution of d , P_D and P_{FA} are,

$$P_D = \int_{d_{min}}^1 \int_{P_{Th}}^{\infty} \frac{1}{\sqrt{2\pi}\sigma_\gamma} e^{-\frac{(P-\mu(x))^2}{2\sigma_\gamma^2}} \frac{1}{D_D} dx dP \quad (18)$$

$$P_{FA} = \int_1^{d_{max}} \int_{P_{Th}}^{\infty} \frac{1}{\sqrt{2\pi}\sigma_\gamma} e^{-\frac{(P-\mu(x))^2}{2\sigma_\gamma^2}} \frac{1}{D_{FA}} dx dP \quad (19)$$

where $\mu(x) = P_{1m} - 10\alpha \log_{10} x$, $D_D = 1 - d_{min}$ and $D_{FA} = d_{max} - 1$. Note that P_D and P_{FA} depend on σ_γ therefore, they have to be calculated for every possible scenario. Fig. 1 shows the probabilities of detection and false alarm as a function of the power threshold for different values of σ_γ^2 . Take into account that there is a trade off between the minimization of P_{FA} and maximization of P_D . In this work we prioritize the minimization of P_{FA} and therefore we select a power threshold value that fulfils $P_{FA} = 5\%$. Note that the P_D is still high, between 82% and 99%.

After detecting the position of interest, the next step is to ensure that the EKF adopts these measurements as position estimations. From equation (11) and taking into account that $\mathbf{H} = \mathbf{I}$ in our design, the estimations will equal the measurements when $\mathbf{K}^{k+1} = \mathbf{I}$, that is,

$$\mathbf{K}^{k+1} = \mathbf{P}_-^{k+1} \mathbf{I}^T (\mathbf{I} \mathbf{P}_-^{k+1} \mathbf{I}^T + \mathbf{R}^{k+1})^{-1} = \mathbf{I} \quad (20)$$

The above condition is fulfilled when the measurement noise covariance matrix is set to zero ($\mathbf{R}^{k+1} = \mathbf{0}$). Assuming \mathbf{R}^{k+1} diagonal, this results also holds if only one sub-block of \mathbf{R}^{k+1} is set to zero. Accordingly, we define the measurement noise

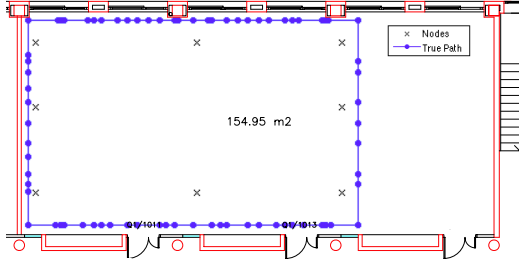


Fig. 2. Scenario 1.

covariance matrix as,

$$\mathbf{R}^{k+1} = \begin{cases} \begin{bmatrix} \epsilon & 0 & 0 & 0 \\ 0 & \epsilon & 0 & 0 \\ 0 & 0 & \sigma_{\hat{V}_k}^2 & 0 \\ 0 & 0 & 0 & \sigma_{\hat{\theta}_k}^2 \end{bmatrix} & \text{if } P_{max} \geq P_{Th} \\ \begin{bmatrix} \sigma_p^2 & 0 & 0 & 0 \\ 0 & \sigma_p^2 & 0 & 0 \\ 0 & 0 & \sigma_{\hat{V}_k}^2 & 0 \\ 0 & 0 & 0 & \sigma_{\hat{\theta}_k}^2 \end{bmatrix} & \text{if } P_{max} < P_{Th} \end{cases} \quad (21)$$

where $\epsilon \ll 1$ (not zero to avoid ill-conditioning problems), σ_p^2 is a standard value of the variance defined by the user and $\sigma_{\hat{V}_k}^2$ and $\sigma_{\hat{\theta}_k}^2$ are respectively the variances of the speed modulus and heading measurements.

In summary, the SCMT-EKF makes it possible to benefit from the short-term high accuracy of the inertial sensors and extend this accuracy over a long period of time.

IV. EXPERIMENTAL VALIDATION

In this section, the proposed method is validated experimentally. We test the performance of the system using the Iris motes from Crossbow. The IMU used is the 9DOF Sensor Stick from Sparkfun which includes a 3 axis accelerometer (ADXL345), a 3 axis magnetometer (HMC5883L) and a 3 axis gyroscope (ITG-3200).

In order to evaluate the performance of the proposed technique, the algorithm is tested in two different scenarios. The first one is a big classroom with an area of 154.95m² and covered with 8 motes as shown in Fig. 2. The true path is a rectangular trajectory of 46.4m length. The second scenario is a long corridor inside a large building. It has an area of 533.12m² (11.2 × 47.6 meters) and it is also covered with 8 motes. The scenario is shown in Fig. 4. The path starts at point A and goes up to B before going back to A. During the path some stops are programmed at these points.

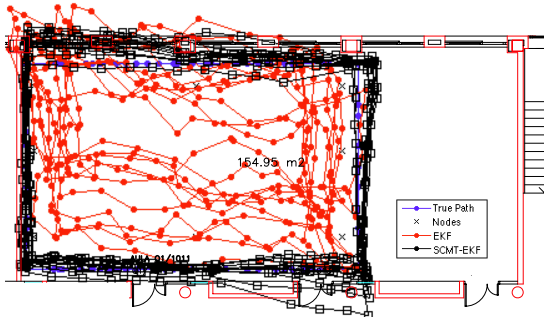


Fig. 3. Estimated Path of the scenario 1.

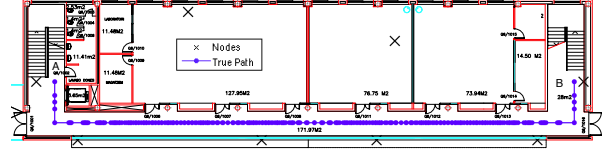


Fig. 4. Scenario 2.

The anchor nodes send a message each second and the mobile node samples the inertial sensors with the following rates: 100Hz for the accelerometer and 15Hz for the magnetometer and gyroscope. Notwithstanding, a measure of \hat{V}_k^k and $\hat{\theta}_k^k$ is computed every second as well. During the experimental validation we compare the results of an EKF configured with the designed SCMT, a reference case with an EKF manually configured and a Least Squares algorithm. In the sequel, these systems are referred to as SCMT-EKF, EKF and LS.

In Fig. 3, the different path estimations for the EKF and the SCMT-EKF filter are shown. Note that the accuracy of the latter is good enough to recognize the trajectory done by the mobile node while this is not possible using the EKF. In order to test the long-term stability of the proposed solution, the trajectory has been repeated several times in several rounds. Note that, in each round, the algorithm is tested during more than 20 minutes. The results show a Root Mean Square Error (RMSE) of 2.8m for the EKF and 1.3m for the proposed technique (SCMT-EKF), which represents an improvement of 53.5%. Finally, we also include the cumulative distribution function (CDF) of the positioning errors in Fig. 5. In this case, we appreciate that the error is below 8m in 90% of occasions for the LS, the error is below 5.8m for the EKF while this error is significantly reduced to 2.3m in the SCMT-EKF.

The results in the second scenario are shown in Fig.6. The tests fulfilled show a RMSE of 2.9m for the EKF and 1.5m for the SCMT-EKF, which represents an improvement of 48.2%. Moreover, Fig.7 shows the CDF for the scenario 2. If we analyse again the error in 90% of the cases we observe that it is situated at 9.5m for the LS, 5.6m for the EKF and 3.3m for the SCMT-EKF.

The experimental validation performed over two different scenarios shows that the proposed indoor tracking system presents a significant improvement on the RMSE with respect to the conventional design. Specially remarkable is that, thanks

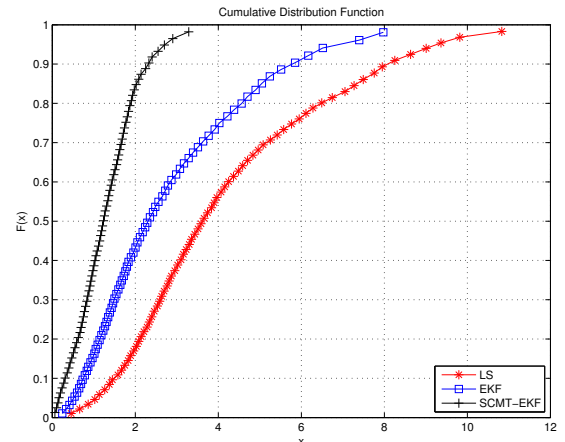


Fig. 5. Cumulative Distributed Function of the error in the Scenario 1.

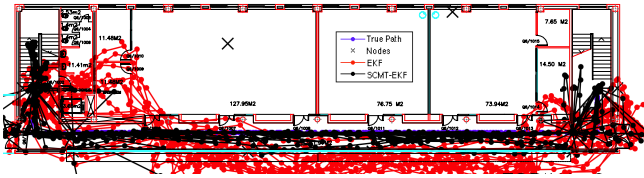


Fig. 6. Estimated Path of the scenario 2.

to the proposed solution, the short-term accuracy of the inertial sensors can be extended in time.

V. CONCLUSION

In this work we present a hybrid indoor positioning system using both RSSI and inertial observations. The system combines position measurements, extracted from the RSSI of a set of anchor nodes, together with velocity measurements (velocity modulus and direction), obtained from an IMU, using an EKF. It is well known that dead reckoning solutions provide good accuracies in the short term but suffer in the long term. In contrast, RSSI-based position estimations are not so accurate but stable in time. In this work, we argue that RSSI measurements can provide accurate position estimates when the mobile node is close enough to an anchor node and we show that we can design a simple EKF-based solution that effectively combines measurements with different degrees of uncertainty. This is achieved with the appropriate configuration of the EKF done by the designed SCMT. Our method defines a noise measurement covariance matrix for every iteration of the EKF based on the statistical characteristics of the position measurements. In this way, the designed system is able to achieve high accuracy not only in the short-term but also in the long-term.

The experimental results prove the validity of the system and show that the RMSE can be reduced up to a 53.5% compared to the conventional EKF. With the proposed system, the trajectory of the person can be better estimated and therefore, it is not only useful for guidance applications but also useful for pattern recognition applications as the ones required, for example, in remote assistance or control. In other words, the good precision achieved and specially the long term stability obtained makes the proposed algorithm a good choice for indoor applications that require the tracking of people.

REFERENCES

- [1] N. Patwari, J. Ash, S. Kyperountas, I. Hero, A.O., R. Moses, and N. Correal, "Locating the nodes: cooperative localization in wireless sensor networks," *Signal Processing Magazine, IEEE*, vol. 22, no. 4, pp. 54 – 69, July 2005.
- [2] A. Boukerche, H. Oliveira, E. Nakamura, and A. Loureiro, "Localization systems for wireless sensor networks," *Wireless Communications, IEEE*, vol. 14, no. 6, pp. 6 –12, December 2007.
- [3] Y. Shen and M. Win, "Fundamental limits of wideband localization; part i: A general framework," *Information Theory, IEEE Transactions on*, vol. 56, no. 10, pp. 4956–4980, 2010.
- [4] Y. Shen, H. Wymeersch, and M. Win, "Fundamental limits of wideband localization; part ii: Cooperative networks," *Information Theory, IEEE Transactions on*, vol. 56, no. 10, pp. 4981–5000, 2010.
- [5] R. Harle, "A survey of indoor inertial positioning systems for pedestrians," *Communications Surveys Tutorials, IEEE*, vol. 15, no. 3, pp. 1281–1293, 2013.

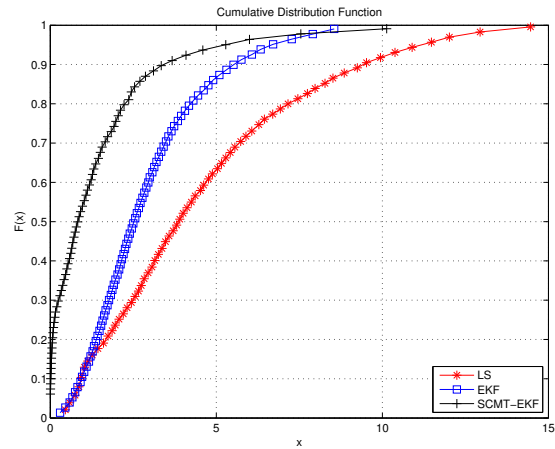


Fig. 7. Cumulative Distributed Function of the error in the Scenario 2.

- [6] E. Foxlin, "Pedestrian tracking with shoe-mounted inertial sensors," *Computer Graphics and Applications, IEEE*, vol. 25, no. 6, pp. 38 – 46, Nov.-Dec. 2005.
- [7] A. Jimenez, F. Seco, C. Prieto, and J. Guevara, "A comparison of pedestrian dead-reckoning algorithms using a low-cost MEMS IMU," in *Intelligent Signal Processing, 2009. WISP 2009. IEEE International Symposium on*, Aug. 2009, pp. 37 –42.
- [8] Q. Ladetto, "On foot navigation: continuous step calibration using both complementary recursive prediction and adaptive Kalman filtering," in *ION GPS/GNSS, 2000 Proceedings of*, Sep. 2000, pp. 1735–1740.
- [9] L. Fang, P. Antsaklis, L. Montestrucque, M. McMickell, M. Lemmon, Y. Sun, H. Fang, I. Koutroulis, M. Haenggi, M. Xie, and X. Xie, "Design of a wireless assisted pedestrian dead reckoning system - the navmote experience," *Instrumentation and Measurement, IEEE Transactions on*, vol. 54, no. 6, pp. 2342 – 2358, Dec. 2005.
- [10] J. Schmid, T. Gadeke, W. Stork, and K. Müller-Glaser, "On the fusion of inertial data for signal strength localization," in *Positioning Navigation and Communication (WPNC), 2011 8th Workshop on*, April 2011, pp. 7 –12.
- [11] A. Correa, A. Morell, M. Barcelo, and J. L. Vicario, "Navigation system for elderly care applications based on wireless sensor networks," in *Signal Processing Conference (EUSIPCO), 2012 Proceedings of the 20th European*, Aug. 2012, pp. 210 –214.
- [12] W. Xiao, W. Ni, and Y. K. Toh, "Integrated wi-fi fingerprinting and inertial sensing for indoor positioning," in *Indoor Positioning and Indoor Navigation (IPIN), 2011 International Conference on*, Sept. 2011, pp. 1 –6.
- [13] L. Klingbeil and T. Wark, "A wireless sensor network for real-time indoor localization and motion monitoring," in *Information Processing in Sensor Networks, 2008. IPSN '08. International Conference on*, April 2008, pp. 39 –50.
- [14] L. Klingbeil, R. Reiner, M. Romanovas, M. Traechtler, and Y. Manoli, "Multi-modal sensor data and information fusion for localization in indoor environments," in *Positioning Navigation and Communication (WPNC), 2010 7th Workshop on*, March 2010, pp. 187 –192.
- [15] K. Frank, B. Krach, N. Catterall, and P. Robertson, "Development and evaluation of a combined wlan & inertial indoor pedestrian positioning system," *ION GNSS, 2009*.
- [16] H. Wymeersch, J. Lien, and M. Win, "Cooperative localization in wireless networks," *Proceedings of the IEEE*, vol. 97, no. 2, pp. 427 –450, Feb. 2009.
- [17] Y. Bar-Shalom, X. R. Li, and T. Kirubarajan, *Estimation with Applications to Tracking and Navigation*, 1st ed. Wiley-Interscience, Jun 2001.
- [18] A. Correa Vila, M. Barcelo, A. Morell, and J. Vicario, "Enhanced inertial-aided indoor tracking system for wireless sensor networks," *Accepted in Sensors Journal, IEEE*, 2014.
- [19] X. Li, "Collaborative localization with received-signal strength in wireless sensor networks," *Vehicular Technology, IEEE Transactions on*, vol. 56, no. 6, pp. 3807–3817, 2007.
- [20] T. S. Rappaport, *Wireless Communications: Principles and Practice*, 1st ed. Piscataway, NJ, USA: IEEE Press, 1996.